© 2010 International Journal of Computer Applications (0975 - 8887)
Volume 1 – No. 15

Modeling, simulation and signal processing for Control room EMI problem using frequency domain Approach and Bayesian estimation

Vidya R. Keshwani
M.E. student, VESIT
D11/2:9, Utkarsha CHS
Sector11, Khanda colony, New Panwel
(W)-410206

Prof. Naveeta Kant
Assistant Professor,
VESIT
Mumbai

Dr. Kallol Roy
M. E. Guide
RRMD, BARC
Mumbai

ABSTRACT
The problem of separation of mixed signal spectrum is encountered in many engineering systems. One such problem is a problem of electromagnetic topology wherein mixed signals at spatial points are encountered and one would like to separate them out using digital signal processing tools. This paper discusses techniques such as fast Fourier transform, short term Fourier transform, wavelet transform and Hilbert Huang transform in light of this application. Advantages and limitations of each technique are bought out for above said problem.

In a computational *EMI* problem, for a given *EM* topology, field values in problem domain can be computed using conventional numerical techniques such as finite difference method, finite element method, etc. However for a real time application, these techniques are of little use as they require large computation time. One would like to have fast computations if on-line real time dynamic error correction is required for quantities being measured. This paper describes one such approach applicable to control room *EMI* problem to obtain best estimates of weak signal being measured in noisy surroundings. The techniques used are Bayesian approaches such as Kalman filter and its variants.

Keywords
Signal, wavelets, Kalman filter.

1. INTRODUCTION
Mixed signal is a signal formed by mixture of arbitrary waves of various amplitudes, frequencies, phases along with noise. These noise can be of varied nature may be Gaussian, non-Gaussian, mixture of several Gaussians, etc. Mixed signal separation is carried out by using various signal separation tools. These inclu-

-de conventional tools such as Fourier transform, Short term Fourier transform, Wavelets, Hilbert transforms and many other advanced transform techniques such as Hilbert Huang transform (*HHT*). In many engineering systems, signal measured can be \

function of one or more physical phenomenon occurring inside system. In other words, sensor signal can be an indicator of various activities taking place inside system under consideration. One would like to separate out these physical phenomenon's which also indicate abnormal situations arising inside a given system. A separation of detector signal essentially aims at finding out all these events happening inside a system.

In a control room having noisy environment, a weak signal arriving from plant on cable gets further corrupted depending on number of *EMI* sources, source strengths and distance of cable from these sources. One would like to evolve a strategy or method to minimize effect of these *EMI* due to these sources on weak signal/s. Further, by measuring *EMI* at various points in a control room, it is possible to correct or compensate for effect of *EMI* into any sensitive equipment placed at a given location. This method of compensation is called as *dynamic error correction*. In order to arrive at the amount of correction to sufficient accuracy, Kalman filters can be used.

Section 2 of paper describes basics of Wavelet transforms and comparisons with Fourier transforms. Section 3 is about *HHT* and section 4 is about basics of Kalman filters and augmented state Kalman filters. Section 5 describes conversion of Maxwell's equations into state space form. Simulations described in section 6 justify *HHT* as better tool for *EMI* signal processing. In addition solution of *EMI* problem in *1D* and *2D* problem domain are also addressed followed by proposed method of *dynamic error correction*.

2. FOURIER TRANSFORMS VS WAVELET TRANSFORM
The Fourier transform's utility lies in its ability to analyze a signal in the time domain for its frequency content. The transform works by first translating a function in the time domain into a function in the frequency domain. The signal can then be analyzed for its frequency content because the Fourier coefficients of the transformed function represent the contribution of each sine and cosine function at each frequency. The discrete Fourier transform (*DFT*) estimates the Fourier transform of a function from a finite number of its sampled points.

The windowed Fourier transform (*WFT*) [9] is one solution to the problem of better representing the non-periodic signal. The *WFT* can be used to give information about signals simultaneously in

the time domain and in the frequency domain. With the *WFT*, the input signal $f(t)$ is chopped up into sections, and each section is analyzed for its frequency content separately. This windowing is accomplished via a weight function that places less emphasis near the interval's endpoints than in the middle. The effect of the window is to localize the signal in time. *WFT* or short time Fourier transform (*STFT*) is defined as in eqn. (1).

(1)

where, $g(t)$ is basis function used for analysis of signal $x(t)$. Continuous wavelet transform (*CWT*) of signal $x(t)$ is defined as,

$$CWT_x(\tau, a) = \frac{1}{\sqrt{|a|}} \int x(t)\Phi^*\left(\frac{t-\tau}{a}\right)dt \qquad (2)$$

Here, $\Phi(t)$ is basis function for *CWT*. The most interesting dissimilarity between these two kinds of transforms is that individual wavelet functions are localized in space however, Fourier sine and cosine functions are not. This localization feature, along with wavelets localization of frequency, makes many functions and operators using wavelets "sparse" when transformed into the wavelet domain. This sparseness, in turn, results in a number of useful applications such as data compression, detecting features in images, and removing noise from time series. Figure 1 shows a *WFT*, where the window is simply a square wave. Because a single window is used for all frequencies in the *WFT*, the resolution of the analysis is the same at all locations in the time-frequency plane.

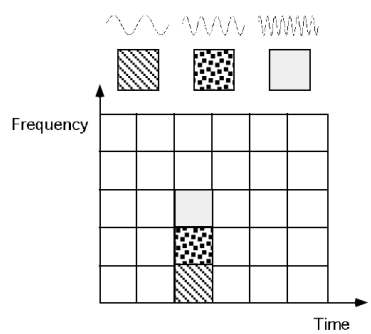

Figure 1. Time frequency analysis using windowed Fourier transforms

An advantage of wavelet transforms is that the windows vary. In order to isolate signal discontinuities, very short basis functions are required while to obtain detailed frequency analysis, very long basis functions are required. A way to achieve this is to have short high-frequency basis functions and long low-frequency ones. This is obtained from wavelet transforms. Figure 2 shows the coverage in the time-frequency plane with wavelet function, the Daubechies wavelet [2].

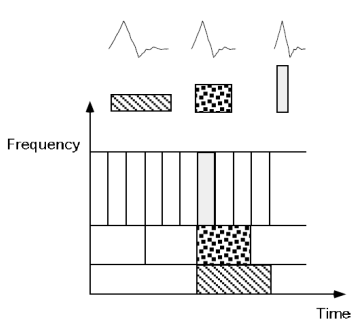

Figure 2. Time frequency analysis using continuous wavelet transforms

WFT cannot handle nonlinear and nonstationery signals. Though wavelets are capable of handling nonstationery signals, their capability to handle nonlinear signals are limited.

2.1 The Sub-band Coding and the Multi-resolution Analysis

The main idea is same as it is in *CWT*. A time-scale representation of a digital signal is obtained using digital filtering techniques. *CWT* is a correlation between a wavelet at different scales and the signal with the scale (or the frequency) being used as a measure of similarity. The continuous wavelet transform is computed by changing the scale of the analysis window, shifting the window in time, multiplying by the signal, and integrating over all times. In the discrete case, filters of different cutoff frequencies are used to analyze the signal at different scales. The signal is passed through a series of high pass filters to analyze the high frequencies, and it is passed through a series of low pass filters to analyze the low frequencies.

The resolution of the signal, which is a measure of the amount of detail information in the signal, is changed by the filtering operations, and the scale is changed by up sampling and down sampling (sub sampling) operations. Sub sampling a signal corresponds to reducing the sampling rate, or removing some of the samples of the signal. The filter bank can be illustrated as in figure 3.

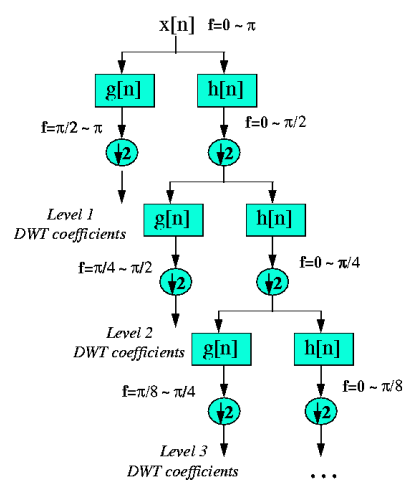

Figure3. The Sub band Coding Algorithm

2.2 APPLICATION TO SYNTHETIC SIGNAL

Synthetic signal comprising of 70 Hz and 750 Hz sine wave with resolution of 20 microseconds with noise added (normally distributed with standard deviation of 0.2882 and zero mean) was generated. Figure 4 shows this generated signal. Figure 5 shows discrete wavelet decomposition of this noisy sine wave. In

uppermost plot, the original sine wave as seen in figure 4. Second plot in figure 5 shows level 3 approximation coefficients (in red) and its comparison with original signal. Third, fourth and fifth plot in figure 5 show the detail coefficient *d3*, *d2* and *d1*. This is wavelet decomposition in time domain using wavelet '*db2*'. Thus, separation can be carried out easily using discrete wavelet decomposition.

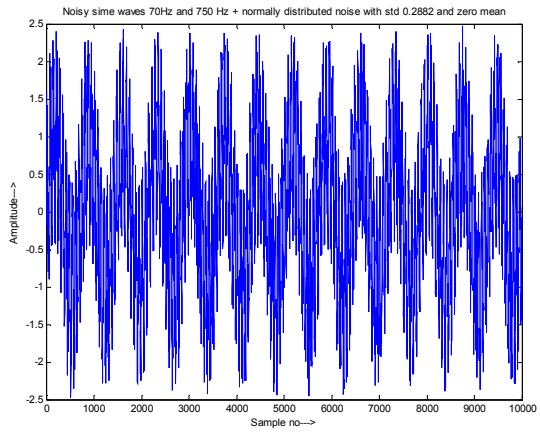

Figure 4. Plot of noisy synthetic signal

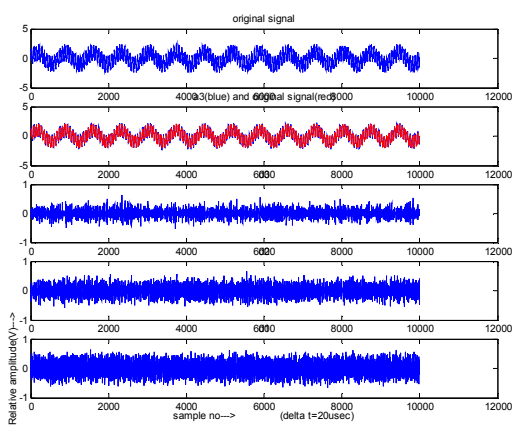

Figure 5. Three level wavelet decomposition using 'db2'

3. INTRINSIC MODE FUNCTIONS, HILBERT HUANG TRANSFORM AND EMPIRICAL MODE DECOMPOSITION

The essence of Empirical mode decomposition (*EMD*) method is to identify the intrinsic oscillatory modes by their characteristic time scales in the data empirically, and then decompose the data accordingly. An intrinsic mode function (*IMF*) represents a simple oscillatory mode as a counterpart to the simple harmonic function, but it is much more general: instead of constant amplitude and frequency, as in a simple harmonic component, the *IMF* can have a variable amplitude and frequency as functions of time. With the above definition for the *IMF*, one can then decompose any function using sifting process [8]. The sifting process serves two purposes: to eliminate riding waves and to make the wave profiles more symmetric. While the first purpose must be achieved for the Hilbert transform to give a meaningful instantaneous frequency, the second purpose must also be achieved in case the neighboring wave amplitudes have too large a disparity. Toward these ends, the sifting process has to be repeated as many times as is required to reduce the extracted signal to an *IMF*. The sifting process can be stopped finally by any of the following predetermined criteria: either when the component or the residue becomes so small that it is less than the predetermined value of substantial consequence, or when the residue becomes a monotonic function from which no more *IMF*s can be extracted.

Thus, a decomposition of the data into n-empirical modes is achieved, and a residue is obtained which can be either the mean trend or a constant. Therefore, total signal $x(t)$ can be represented as,

$$x(t) = \sum_{j=1}^{n} c_j + r_n \tag{3}$$

Contrary to almost all the previous methods, this new method is intuitive, direct, a posteriori and adaptive, with the basis of the decomposition based on, and derived from the data. A comparative summary of Fourier, wavelet and *HHT* analysis is given in table 1. This table shows that the *HHT* is indeed a powerful method for analyzing data from nonlinear and non-stationary processes. It is based on an adaptive basis and the frequency is derived by differentiation rather than convolution. Therefore, it is not limited by the uncertainty principle. It is applicable to nonlinear and non-stationary data and presents the results in time-frequency-energy space for feature extraction.

Table 1. Comparison of capabilities of Fourier, Wavelet and Hilbert transform

	Fourier	Wavelet	Hilbert
Basis	apriori	apriori	adaptive
Frequency	Global uncertainty	Regional uncertainty	Local uncertainty
Presentation	energy-frequency	energy-time-frequency	energy-time-frequency
Nonlinear	no	no	yes
Nonstationary	no	yes	yes
Feature extraction	no	discrete: no, continuous: yes	yes
Theoretical base	theory complete	theory complete	empirical

4. KALMAN FILTER AND BAYESIAN ESTIMATION

A Kalman filter is an optimal recursive data processing algorithm. It processes all available measurements, regardless of their precision, to estimate the current value of the variable/s of interest, with use of,

1) Knowledge of the system and measurement device dynamics.
2) The statistical description of the system noises, measurement errors, and uncertainty in the dynamics models and
3) Any available information about initial condition of the variables of interest.

Rather than ignore any of the outputs from system, a Kalman filter could be built to combine all of this data and knowledge of the various system dynamics to generate an overall best estimate of states of system [7, 5, 1]. Often the variables of interest, some finite number of quantities to describe the state of the system, cannot be measured directly, and some means of inferring these values from the available data must be generated. For instance, an air data system directly provides static and pitot pressure, from which velocity must be inferred. This inference is complicated by the fact that the system is typically driven by inputs other than known controls and that the relationships among the various state variables and measured outputs are known only with some degree of uncertainty. Furthermore, any measurement will be corrupted to some degree by noise, biases and device inaccuracies, and so a means of extracting valuable information from a noisy signal must be provided as well. There may also be a number of different measuring devices, each with its own particular dynamics and error characteristics that provide some information about a particular variable, and it would be desirable to combine these outputs in a systematic and optimal manner. A Kalman filter combines all available measurement data, plus prior knowledge about the system and measuring devices, to produce an estimate of the desired variables in such a manner that the error is minimized statistically. There are many means of accomplishing this objective. If a *Bayesian viewpoint* is adopted, than the filter propagates the conditional probability density of the desired quantities, conditioned on knowledge of the actual data coming from the measuring devices. The set of measurement data **z** will be assumed to be a linear combination of the variables of interest (say **X**), corrupted by an uncertain measurement disturbance **v** of dimension *m*:

$$\mathbf{z} = \mathbf{HX} + \mathbf{v}$$

where, **H** is known *m* by *n* matrix. Let **v** be a Gaussian random variable characterized by mean **0** and covariance **R**, and assume that **v** and **X** are independent. State space model of system can now be represented as,

$$\dot{\mathbf{X}}(t) = \mathbf{F}(t)\mathbf{X}(t) + \mathbf{B}(t)\mathbf{u}(t) + \mathbf{G}(t)\mathbf{w}(t) \tag{4}$$

$$\mathbf{z}(t_i) = \mathbf{H}(t_i)\mathbf{X}(t_i) + \mathbf{v}(t_i) \tag{5}$$

where $\mathbf{X}(t)$ is the system state, $\mathbf{w}(t)$ and $\mathbf{v}(t_i)$ are white Gaussian noises, assumed independent of each other and of initial condition $\mathbf{X}(t_0) = \mathbf{X}_0$, where $\mathbf{X}_0$ is a Gaussian random variable. These noises model not only the disturbances and noise corruption that affect the system, but also the uncertainty inherent in the mathematical models themselves. It is desired to combine the measurement data taken from the actual system with the information provided by the system model and statistical description of uncertainties, in order to obtain an optimal estimate of the system state. The optimal state estimate is propagated from measurement time t_{i-1} to measurement time t_i by the relation,

$$\hat{\mathbf{X}}(t_i^-) = \phi(t_i, t_{i-1})\hat{\mathbf{X}}(t_{i-1}^+) + \int_{t_{i-1}}^{t_i} \phi(t_i, \tau)\mathbf{B}(\tau)\mathbf{u}(\tau)d\tau \tag{6}$$

$$\mathbf{P}(t_i^-) = \boldsymbol{\phi}(t_i, t_{i-1})\mathbf{P}(t_{i-1}^+)\boldsymbol{\phi}^T(t_i, t_{i-1}) + \int_{t_{i-1}}^{t_i} \boldsymbol{\phi}(t_{i+1}, \tau)\mathbf{G}(\tau)\mathbf{Q}(\tau)\mathbf{G}^T(\tau)\boldsymbol{\phi}^T(t_{i+1}, \tau)d\tau \tag{7}$$

Here, $\boldsymbol{\phi}(t_i, t_{i-1})$ is state transition matrix, $\mathbf{P}(t_i^-)$ is *apriori* state error covariance, **Q** is covariance in state noise **w** with **G** as its strength. At measurement time t_i, the measurement $\mathbf{z}_i$ becomes available. The estimate is updated by defining the Kalman filter gain $\mathbf{K}(t_i)$ and employing it in both mean and covariance relations [7]. Then,

$$\mathbf{K}(t_i) = \mathbf{P}(t_i^-)\mathbf{H}^T(t_i)\left[\mathbf{H}(t_i)\mathbf{P}(t_i^-)\mathbf{H}^T(t_i) + \mathbf{R}(t_i)\right]^{-1} \tag{8}$$

$$\hat{\mathbf{X}}(t_i^+) = \hat{\mathbf{X}}(t_i^-) + \mathbf{K}(t_i)\left[\mathbf{z}_i - \mathbf{H}(t_i)\hat{\mathbf{X}}(t_i^-)\right] \tag{9}$$

$$\mathbf{P}(t_i^+) = \mathbf{P}(t_i^-) - \mathbf{K}(t_i)\mathbf{H}(t_i)\mathbf{P}(t_i^-) \tag{10}$$

Here, $\hat{\mathbf{X}}(t_i^+)$ is posteriori state estimate and $\mathbf{P}(t_i^+)$ is posteriori state error covariance. The initial conditions for recursion are given by,

$$\hat{\mathbf{X}}(t_0) = E\left[\mathbf{X}(t_0)\right] = \hat{\mathbf{X}}_0 \tag{11}$$

$$\mathbf{P}(t_0) = E\left\{\left[\mathbf{X}(t_0) - \hat{\mathbf{X}}_0\right]\left[\mathbf{X}(t_0) - \hat{\mathbf{X}}_0\right]^T\right\} = \mathbf{P}_0 \tag{12}$$

Figure 6 shows the block diagram of Kalman filter.

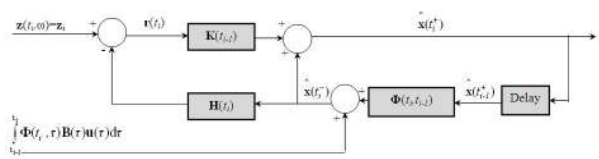

Figure 6. Sampled data Kalman filter block diagram

4.1 Discrete Kalman filter

The Kalman filter estimates state of a process by using a form of feedback control: the filter estimates the process state at some time and then obtains feedback in the form of (noisy) measurements. The equations for the Kalman filter fall into two groups: time update equations and measurement update equations. The time update equations are responsible for projecting forward (in time) the current state and error covariance estimates to obtain the apriori estimates for the next time step. The measurement update equations are responsible for the feedback i.e., for incorporating a new measurement into the apriori estimate to obtain an improved aposteriori estimate. The time update equations can also be thought of as predictor equations, while the measurement update equations can be thought of as corrector equations. Indeed the final estimation algorithm resembles that of a predictor-corrector algorithm for solving numerical problems as shown in figure 7.

Converting eqn. (6) to eqn. (10) into discrete form by replacing t_i, by *k* and t_{i-1},by *k-1*, the following set of time update equations (13) and (14) and measurement update equations (15), (16) and (17) are obtained.

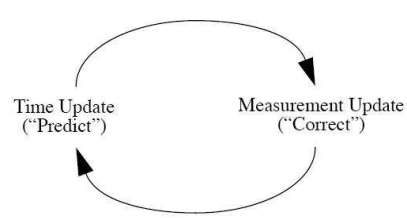

Figure 7. The ongoing discrete Kalman filter cycle

$$\hat{\mathbf{X}}_k = \mathbf{A}_{k,k-1}\hat{\mathbf{X}}_{k-1} + \mathbf{B}_{k,k-1}\mathbf{u}_{k-1} \tag{13}$$

$$\mathbf{P}_k = \mathbf{A}_{k,k-1}\mathbf{P}_{k-1|k-1}\mathbf{A}_{k,k-1}^T + Q \tag{14}$$

$$\mathbf{K}_k = \mathbf{P}_{k|k-1}\mathbf{H}_k^T\left[\mathbf{H}_k\mathbf{P}_{k|k-1}\mathbf{H}_k^T + \mathbf{R}_k\right]^{-1} \tag{15}$$

$$\mathbf{P}_{k|k} = \mathbf{P}_{k|k-1} - \mathbf{K}_k\mathbf{H}_k\mathbf{P}_{k|k-1} \tag{16}$$

$$\hat{\mathbf{X}}_{k|k} = \mathbf{A}_{k,k-1}\hat{\mathbf{X}}_{k-1|k-1} + \mathbf{K}_k\left(\mathbf{z}_k - \mathbf{H}_k\mathbf{A}_{k,k-1}\hat{\mathbf{X}}_{k-1|k-1}\right) \tag{17}$$

The symbols have equivalent meanings as described previously. Figure 8 offers a complete picture of the operation of the filter.

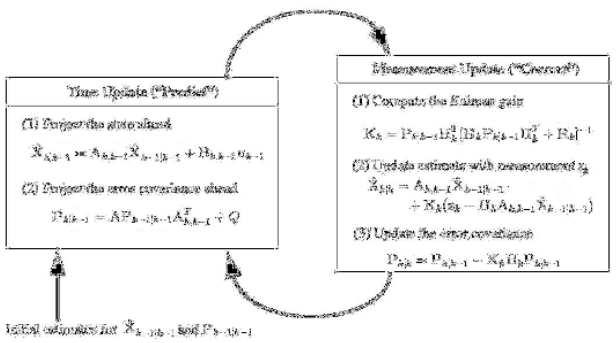

Figure 8: A complete picture of the operation of the filter

4.2 Augmented state Kalman filter

In many instances, the state space model contains parameters which may deviate by constant but unknown amounts from their nominal values. Use of the nominal values of the parameters in the filter design leads to unacceptably large errors in the estimate provided by the filter [4]. To reduce the estimation errors which could arise from such incorrect modeling, it is a common practice to augment the state vector of the original problem by adding additional components to represent the uncertain parameters, which are conveniently designated as bias terms. The filter then estimates the bias terms as well as those of the original problem. This method is reasonably effective when the number of bias terms is small relative to the state variables of the original problem; the dimension of the state vector is then not significantly increased by adjoining the state variables which are used to represent the bias terms. The recursive algorithm for augmented state Kalman filter is almost same as that for Kalman filter with modifications that it estimates bias and its covariance.

5. CONVERSION OF N-DIMENSIONAL MAXWELL'S EQUATION INTO STATE SPACE FORM

To address an *EMI* problem, let us consider Maxwell's equations [12, 3],

$$\nabla \times \mathbf{E} = \frac{\partial \mathbf{B}}{\partial t} \tag{18}$$

$$\nabla \times \mathbf{H} = \mathbf{J} + \frac{\partial \mathbf{D}}{\partial t} \tag{19}$$

$$\nabla \bullet \mathbf{D} = \rho_{\mathcal{V}} \tag{20}$$

$$\nabla \bullet \mathbf{B} = 0 \tag{21}$$

Here, **E** is electric field strength, **B** is magnetic flux density, **D** is electric flux, **H** is magnetic field strength, **J** is current density and $\rho_{\mathcal{V}}$ is volume charge density. Along with above four Maxwell's equations, following three constitutive relations are required.

$$\mathbf{J} = \sigma\mathbf{E} \tag{22}$$

$$\mathbf{D} = \varepsilon\mathbf{E} \tag{23}$$

$$\mathbf{B} = \mu\mathbf{H} \tag{24}$$

Here, σ, ε and μ are conductivity, permittivity and permeability of medium respectively. Assume electric field is in y-direction and magnetic field is in z-direction. It is possible to convert four Maxwell's equations (for 1D case) into form [6],

$$\frac{\partial}{\partial t}\begin{pmatrix} \dfrac{\partial e(x,t)}{\partial t} \\ \dfrac{\partial b(x,t)}{\partial t} \end{pmatrix} = \begin{pmatrix} -\dfrac{\sigma}{\varepsilon} & 0 \\ 0 & -\dfrac{\sigma}{\varepsilon} \end{pmatrix}\begin{pmatrix} \dfrac{\partial e(x,t)}{\partial t} \\ \dfrac{\partial b(x,t)}{\partial t} \end{pmatrix} + \begin{pmatrix} \dfrac{1}{\mu\varepsilon} & 0 \\ 0 & \dfrac{1}{\mu\varepsilon} \end{pmatrix}\begin{pmatrix} \dfrac{\partial^2 e(x,t)}{\partial x^2} \\ \dfrac{\partial^2 b(x,t)}{\partial x^2} \end{pmatrix} \tag{25}$$

If, $\mathbf{X} = \begin{pmatrix} \dfrac{\partial e(x,t)}{\partial t} \\ \dfrac{\partial b(x,t)}{\partial t} \end{pmatrix}$, $\boldsymbol{A} = \begin{pmatrix} -\dfrac{\sigma}{\varepsilon} & 0 \\ 0 & -\dfrac{\sigma}{\varepsilon} \end{pmatrix}$

$$\boldsymbol{B} = \begin{pmatrix} \dfrac{1}{\mu\varepsilon} & 0 \\ 0 & \dfrac{1}{\mu\varepsilon} \end{pmatrix}, \mathbf{u} = \begin{pmatrix} \dfrac{\partial^2 e(x,t)}{\partial x^2} \\ \dfrac{\partial^2 b(x,t)}{\partial x^2} \end{pmatrix}$$

then eqn. (25) can be written in standard state space form,

$$\dot{\mathbf{X}} = \boldsymbol{A}\mathbf{X} + \boldsymbol{B}\mathbf{u} \tag{26}$$

Hence, by applying standard state space equation solution techniques one can solve electromagnetic field problem. It is possible to extend eqn. (25) to *2D* case by replacing $\dfrac{\partial^2}{\partial x^2}$ by $\left(\dfrac{\partial^2}{\partial x^2} + \dfrac{\partial^2}{\partial y^2}\right)$. For extending to *3D* case, replace it by $\left(\dfrac{\partial^2}{\partial x^2} + \dfrac{\partial^2}{\partial y^2} + \dfrac{\partial^2}{\partial z^2}\right)$.

6. SIMULATION RESULTS

Assume a *1D* problem with dominance of magnetic field. Since eqn. (25) has second partial derivative with respect to spatial

variable x, in order to find out $B(x,t)$ knowledge of **B** is needed as function of spatial co-ordinates x. As per Biot's Savart's law, **B** at any point at distance r away from source varies inversely proportional to r^2. Hence for ith sinusoidal source having unity strength and frequency ω_i, input to state space eqn. (25) becomes,

For a 1D case,

$$u_i = \frac{\partial^2}{\partial x^2}\left(\frac{\sin(\omega_i t)}{x^2}\right)$$

$$= 6\left(\frac{\sin(\omega_i t)}{x^4}\right)$$

For a 2D case,

$$u_i = \left(\frac{\partial^2}{\partial x^2} + \frac{\partial^2}{\partial y^2}\right)\left(\frac{\sin(\omega_i t)}{x^2 + y^2}\right) = 6\left(\frac{\sin(\omega_i t)}{x^4 + y^4}\right)$$

For a 3D case,

$$u_i = \left(\frac{\partial^2}{\partial x^2} + \frac{\partial^2}{\partial y^2} + \frac{\partial^2}{\partial z^2}\right)\left(\frac{\sin(\omega_i t)}{x^2 + y^2 + z^2}\right)$$

$$= 6\left(\frac{\sin(\omega_i t)}{x^4 + y^4 + z^4}\right)$$

Since σ, ε and μ are known, matrices ***A*** and ***B*** are known.

6.1 Application of *HHT* to a *1D* problem of electromagnetic topology

Problem statement: Amidst multiple *EMI* sources, determine co-ordinates at which minimum **E** field or **B** field exists so that sensitive equipment can be placed there. Also, determine the frequency contents of signal so that susceptibility of equipment to each frequency can be determined. Limiting to *1D* case (i.e., collinear **B** field sources), consider three sources. First one with excitation as 10 *Hz* sine wave, second one with quadratic chirp excitation from 5 *Hz* to 50 *Hz*, while third one has excitation as 80 *Hz*. Time domain signals can be seen in figure 9. The strength of **B** field at various locations in *1D* problem can be found out by solving state space eqn. (26). The result can be seen in form of figure 10.

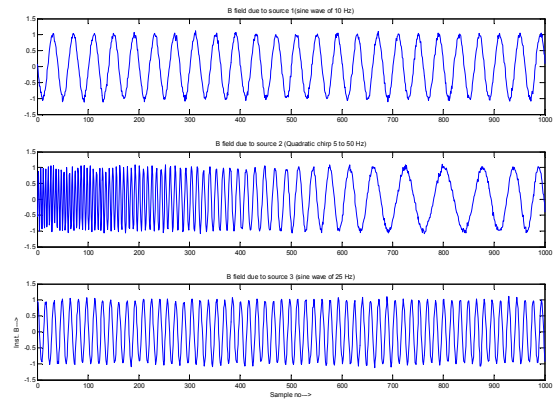

Figure 9. Time domain source excitation signals for EMI problem

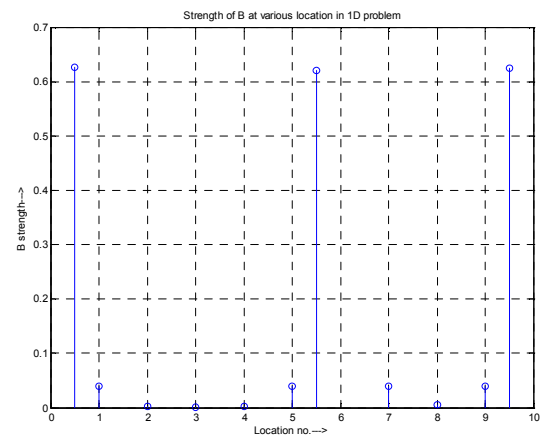

Figure 10. Strength of B field at various locations

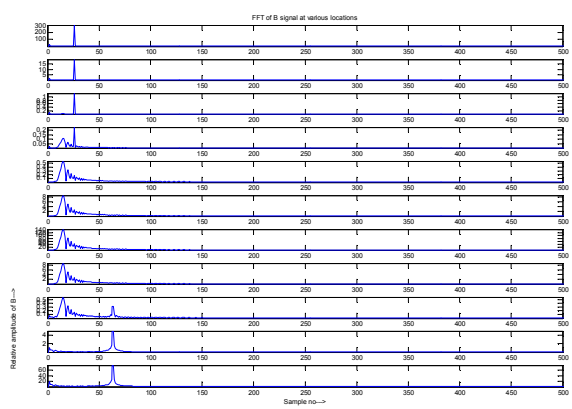

Figure 11. FFT of B field signal at various locations

The *FFT* plot shown in figure 11 does not provide any significant information about frequency content at each location especially about non-stationarity of one of the sources. *HHT* applied to **B** field signal near source 1 results in Hilbert spectrum as seen in figure 12.

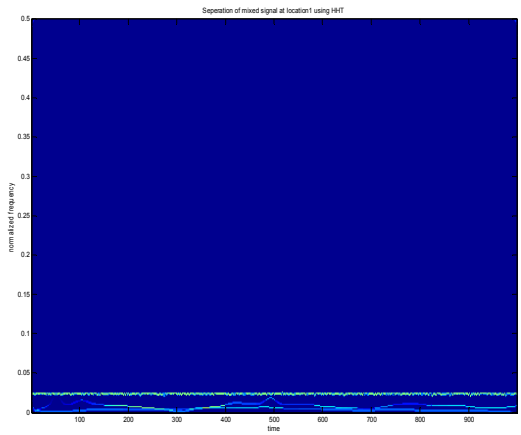

Figure 12. HHT spectrum of B field signal at location near source 1

HHT applied to **B** field signal between source1 and source2 results in Hilbert spectrum as seen in figure 13. For comparison purpose, figure 14 shows spectrogram of **B** field signals at same location as in figure 13. Clearly, it can be seen that unlike *FFT*, *HHT* is able to show clearly the presence of stationary as well as non-stationary components in mixed signal at this location.

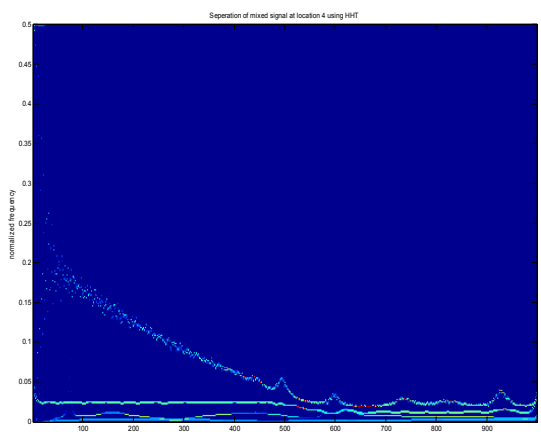

Figure13. HHT spectrum of B field signal at location between source 1 and source 2

6.2 Application to a *2D* problem of electromagnetic topology

Limiting problem to *2D* case and solving state space eqn. (26), gives $\frac{\partial \mathbf{B}}{\partial t}$, integration of which gives $B(x,y,t)$. Thus, **B** field

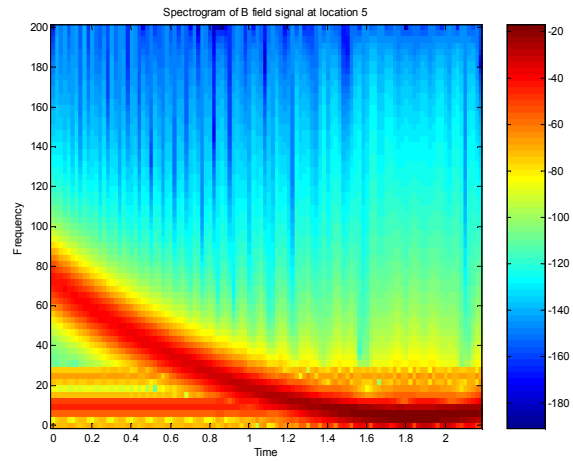

Figure14. Spectrogram of B field signal at location between source 1 and source 2

distribution in *2D* problem domain can be determined. This can be better understood by following *2D* example problem. Consider four *EMI* sources placed as in figure 15 having magnetic dominance, each emitting sinusoidal magnetic field of different strength but of known value. Assume that source S2 has highest strength among all four sources.

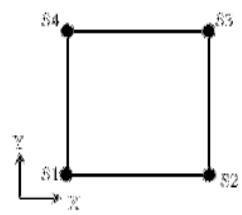

Figure 15. Problem domain for an EMI topology problem

Solution of **B** field at various spatial points gives **B** field distribution as seen in figure 16. These simulations give two important information: Firstly, it is possible to determine point of minimum **B**, thus optimal positional placement of sensitive equipments can be determined easily. Secondly, if a sensitive instrument is placed at any point (x,y) amidst these *EMI* sources, an online solution of eqn. (25) for a known strength of all sources can be estimated. Hence, a correction signal can be generated for this instrument reading. Note that solution of state space equation given by eqn. (26), does not require high amount of computations as is required by conventional finite element method (*FEM*), finite difference method (*FDM*), etc [10]. Thus, this method works in favor of real time implementation. The process of *dynamic error correction* can be understood from figure 17. The correction estimated by this method needs to be accurate enough to correct for instrument reading. Often, there is an uncertainty associated with ***A*** and ***B*** matrices of eqn. (26) due to uncertainty or time varying nature of media properties (σ, ε and μ in present case). These uncertainties [11] can be modeled as noise terms and hence Kalman filter algorithm is useful here. Thus, solving state space model eqn. (26) by Kalman filter algorithm given by equations (13) to (17) gives an accurate estimate of $B(x,y,t)$, thus giving an accurate error compensation.

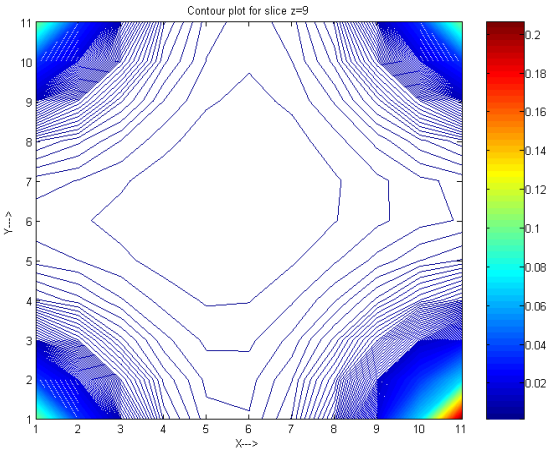

Figure 16. B field distribution for an EMI topology problem

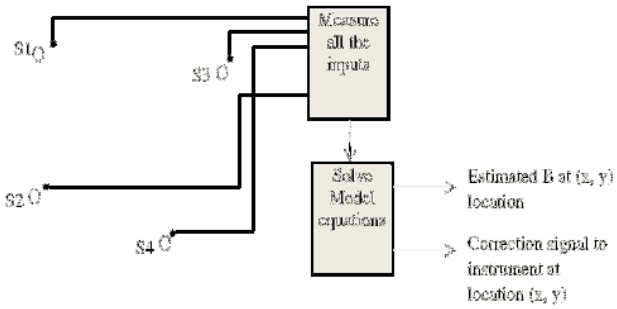

Figure 17. B field distribution for an EMI topology problem

Such strategy cannot be implemented by conventional numerical method based solutions as they require large computation time due to intense computations they carry out. Such limitation does not arise for solution of state space equation for Maxwell's equations (i.e., eqn. (25) which aims at solving for **B** field only at desired location.

7. CONCLUSIONS

The combination of the empirical mode decomposition (*EMD*) method and the associated Hilbert spectral analysis has offered a powerful method for nonlinear and non-stationary data analysis. Central to the present approach is the sifting process to produce the *IMF*s, which enables complicated data analysis. The expansion in terms of the *IMF* basis has the appearance of a generalized Fourier analysis with variable amplitudes and frequencies. It is local and adaptive method in frequency time analysis. A great advantage of *EMD* and Hilbert spectral analysis is the effective use of the data. The advantages were illustrated through a problem of signal separation encountered in electromagnetic interference topology determination.

Kalman filter is a tool which works as an estimator given a model describing the underlying phenomenon which generates the signal to be estimated. More general estimators are augmented state Kalman filters which take care of bias present in any of states of a system under consideration. It is possible to express Maxwell's equations into state space form. The solution of EM topology problem, gives confidence that this conversion is valid. Since Kalman estimation relies on existence of process model, this conversion is useful. The application mentioned in this paper proposed that it is possible to use the state space model of Maxwell's equations along with Kalman filter algorithm to carry out dynamic error correction for sensitive signals arriving in a noisy control room.

8. ACKNOWLEDGMENTS

Authors would like to acknowledge Dr. Kallol Roy, Scientific officer, Bhabha Atomic research center (BARC), Mumbai, who is M. E. guide to author no. 1.

9. REFERENCES

[1] Brown, R. G.,P. Y. C. Hwang., Introduction to Random Signals and Applied Kalman Filtering, John Wiley and Sons, Inc, 1992.

[2] I. Daubechies, “Orthonormal Bases of Compactly Supported Wavelets”, Comm. Pure Appl. Math, Vol. 41, 1988.

[3] Daniel Fleisch, A Student’s Guide to Maxwell’s Equations, Cambridge University Press , 2008

[4] Bernard Friedland, “Treatment of Bias in Recursive Filtering”, IEEE Transactions on Automatic control, AC-14 no. 4, August 1969, pp. 359-367.

[5] Gelb, A., Applied Optimal Estimation, MIT Press, Cambridge, MA, 1974.

[6] John E. Gray, Ronald E. Helmick, “A state space approach to determining solution to Maxwell’s for a one-dimensional dispersive medium”, IEEE proc. Elec. Comp, 1991.

[7] Peter S. Maybeck, Stochastic models, estimation and control", Academic Press, New York, 1979.

[8] Norden E. Huang, Zheng Shen, Steven R. Long, Manli C. Wu, Hsing H. Liu Shih, Quanan Zheng, Nai-Chyuan Yen, Chi Chao Tung8 and Henry H. Liu, “The empirical mode decomposition and the Hilbert spectrum for nonlinear and nonstationary time series analysis”, Proc. of IR. Soc. Lond. A, October 1998 454, pp. 903-955.

[9] Olivier Rioul and Martin Vetterlli, “Wavelets and signal processing”, IEEE transactions on signal processing, October 1991, pp. 5-6.

[10] Dragan Poljak, Advanced modeling in computational electromagnetic compatibility, Wiley Interscience A John Wiley Sons, Inc., Publication.

[11] George M. Siouris, An engineering approach to optimal control and estimation theory, A Wiley Interscience publication John Wiley and Sons Inc New York.

[12] William H. Hayt, John A. Buck, Engineering electromagnetics, 4th edition.